

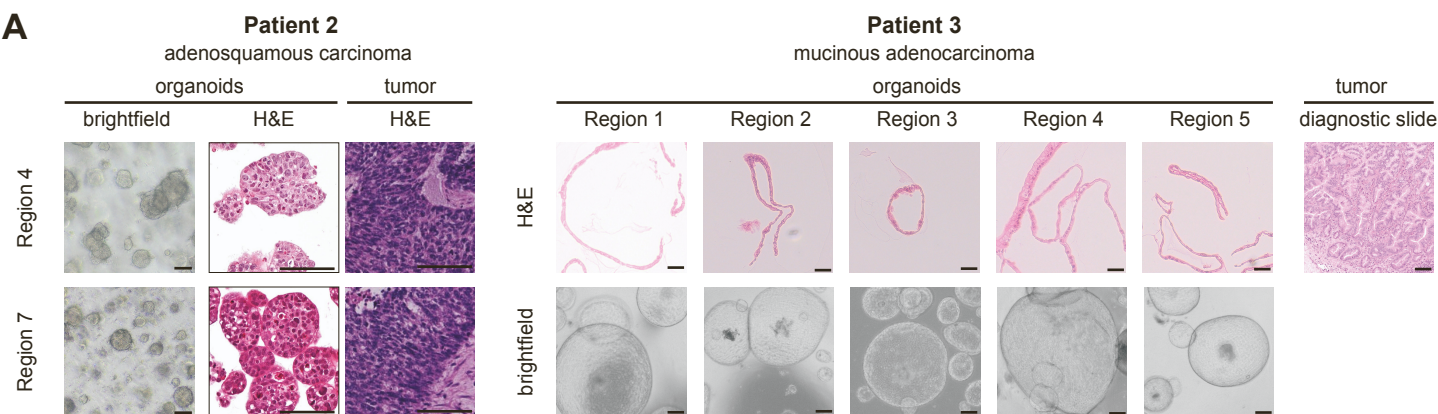
Supplemental information

Subclonal immune evasion in non-small cell lung cancer

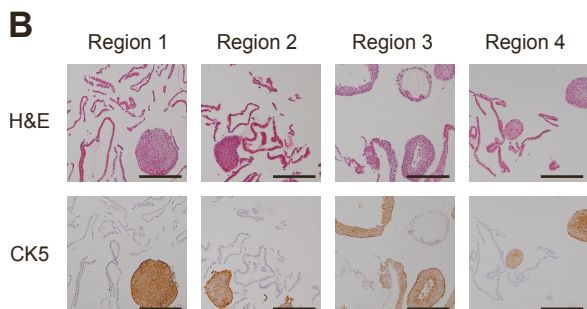
Krijn K. Dijkstra, Roberto Vendramin, Despoina Karagianni, Maartje Witsen, Felipe Gálvez-Cancino, Mark S. Hill, Kane A. Foster, Vittorio Barbè, Mihaela Angelova, Robert E. Hynds, David R. Pearce, Carlos Martínez-Ruiz, James R.M. Black, Ariana Huebner, Oriol Pich, Andrew Rowan, Marcellus Augustine, Clare Puttick, David A. Moore, Lydia L. Liu, Sadegh Saghafinia, Joris van de Haar, Selvaraju Veeriah, Cristina Naceur-Lombardelli, Antonia Toncheva, Supreet Kaur Bola, Crispin T. Hiley, Mariam Jamal-Hanjani, Nicholas McGranahan, Kevin Litchfield, James L. Reading, Benny Chain, TRACERx consortium, Sergio A. Quezada, Emile E. Voest, and Charles Swanton

Figure S1

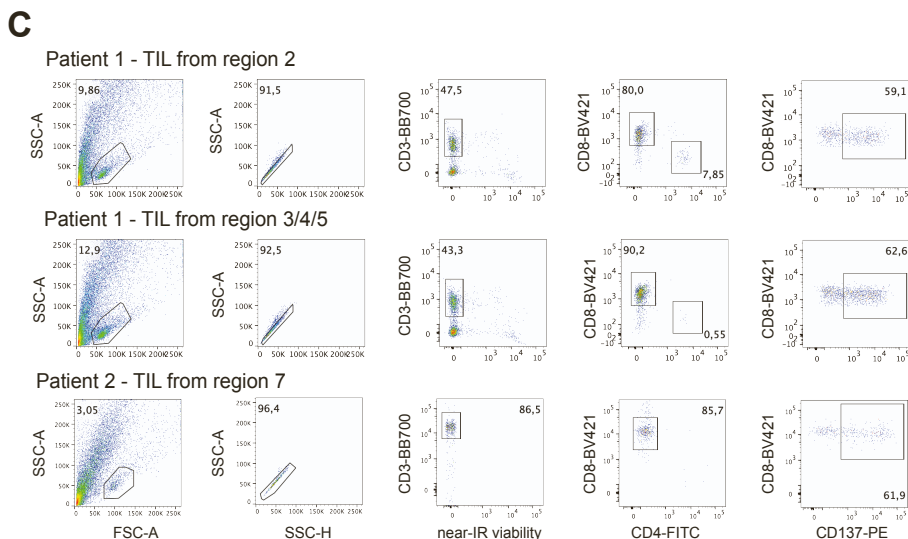
A



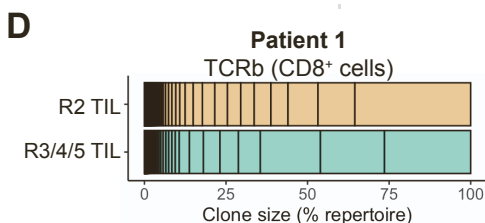
B



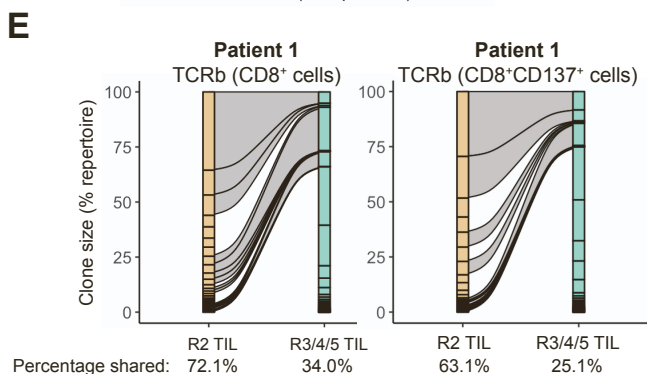
C



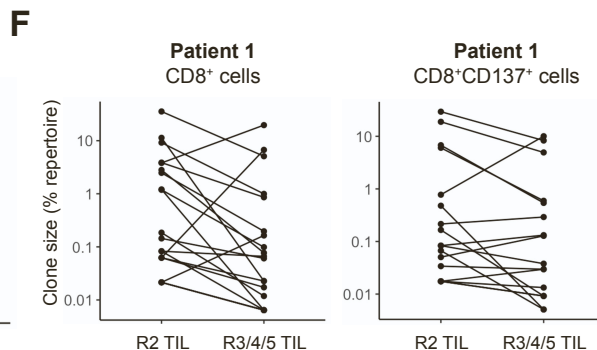
D



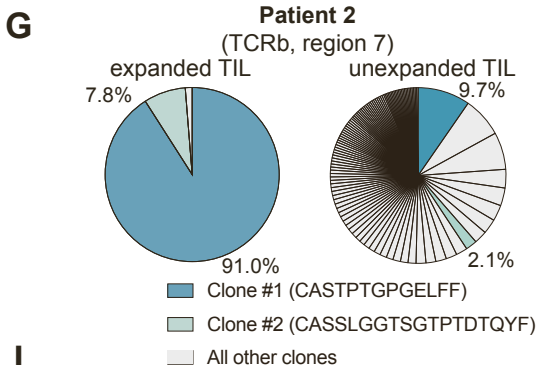
E



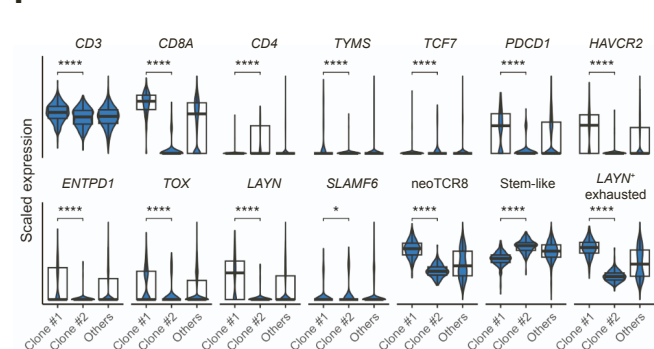
F



G



I



H

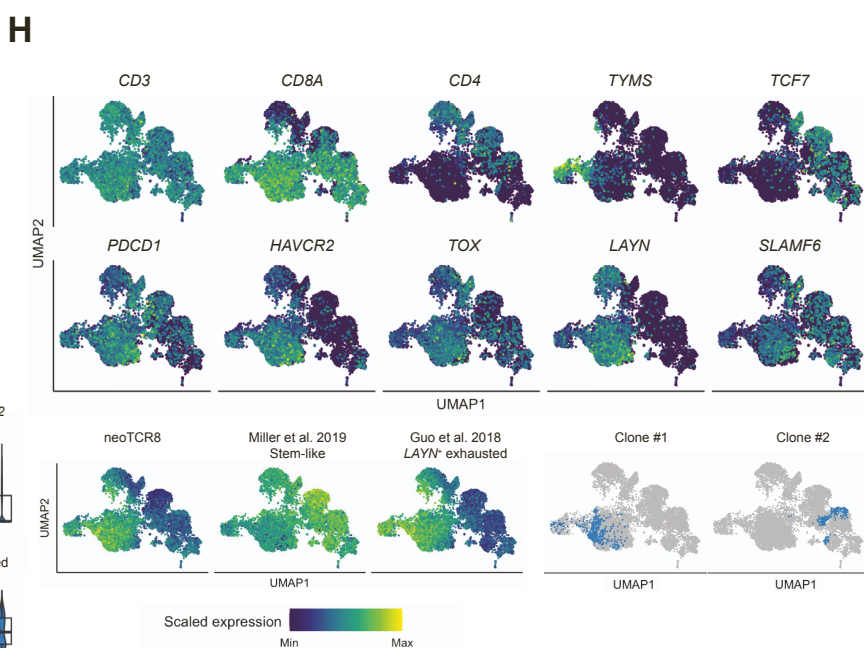


Figure S1. Histomorphology of primary tumors and corresponding organoids and T cell receptor sequencing of unexpanded and expanded TIL, related to Figures 1 and 2 and STAR* Methods.

- A) Brightfield microscopy images and hematoxylin and eosin (H&E) stained slides of regional tumor organoids and corresponding tumor regions from patients 2 and 3. For the original tumor from patient 3 no regional slides were available. Scale bar: 100 μ m.
- B) Slides of patient 3 organoids stained with H&E or cytokeratin 5 (CK5) prior to isolation of pure CK5-tumor organoids. Scale bar: 100 μ m.
- C) Gating strategy. Each panel is subset on cells falling in the gate in panel to the left. Numbers indicate percentage of cells of parent population. FSC-A: forward scatter area; SSC-A: side scatter area; SSC-H: side scatter height.
- D) TCRb repertoire of expanded CD8⁺ TIL from either region 2 (n = 4888), or combined regions 3/4/5 from patient 1 (n = 18412).
- E) Overlap in TCRb repertoire between expanded CD8⁺ TIL products originating either from region 2, or combined regions 3/4/5 for CD8⁺ (left) or CD8⁺CD137⁺ tumor-reactive cells upon organoid co-culture (right) from patient 1. Proportion of repertoire shared between TIL sources indicated. N = 4888 (R2, CD8⁺), 18412 (R3/4/5, CD8⁺), 6069 (R2, CD8⁺CD137⁺), 24418 (R3/4/5, CD8⁺CD137⁺).
- F) Proportion of individual clones found in both TIL products (from region 2, or region 3/4/5 combined) as percentage of unselected (CD8⁺) or tumor-reactive (CD8⁺CD137⁺) TIL repertoire.
- G) Comparison of TCRb abundance in unexpanded (n = 1417) or expanded TIL (n = 52590) from region 7 (patient 2). Clones with >3 counts are plotted. Dominant and subdominant clones in expanded TIL are color coded in both pie charts.
- H) Unifold manifold approximation and projection (UMAP) showing scaled expression of indicated genes, as well as a neoantigen-specific CD8⁺ T cell score (neoTCR8¹), stem-like signature² and exhausted signature³ in combined single cell RNA and TCR sequencing data of unexpanded TIL from patient 7 (n = 8744). Expression of TCRs corresponding to clone #1 or #2 is indicated. Heat maps indicate scaled minimal and maximum expression per gene or signature.
- I) Scaled expression of genes and signatures from panel E in clone #1 (n = 426 cells), #2 (n = 218 cells) or all other clones (n = 8110 cells) in unexpanded TIL from patient 2 (region 7). Unpaired Wilcoxon test. Box plots show interquartile range (IQR, 25th to 75th percentile) and horizontal bar shows median expression. Whiskers show lowest (or highest) value within 1.5x of the IQR below the 25th (bottom) or above the 75th (top) percentile. Asterisks indicate significance: * P < 0.05; **** P < 0.0001.

Figure S2

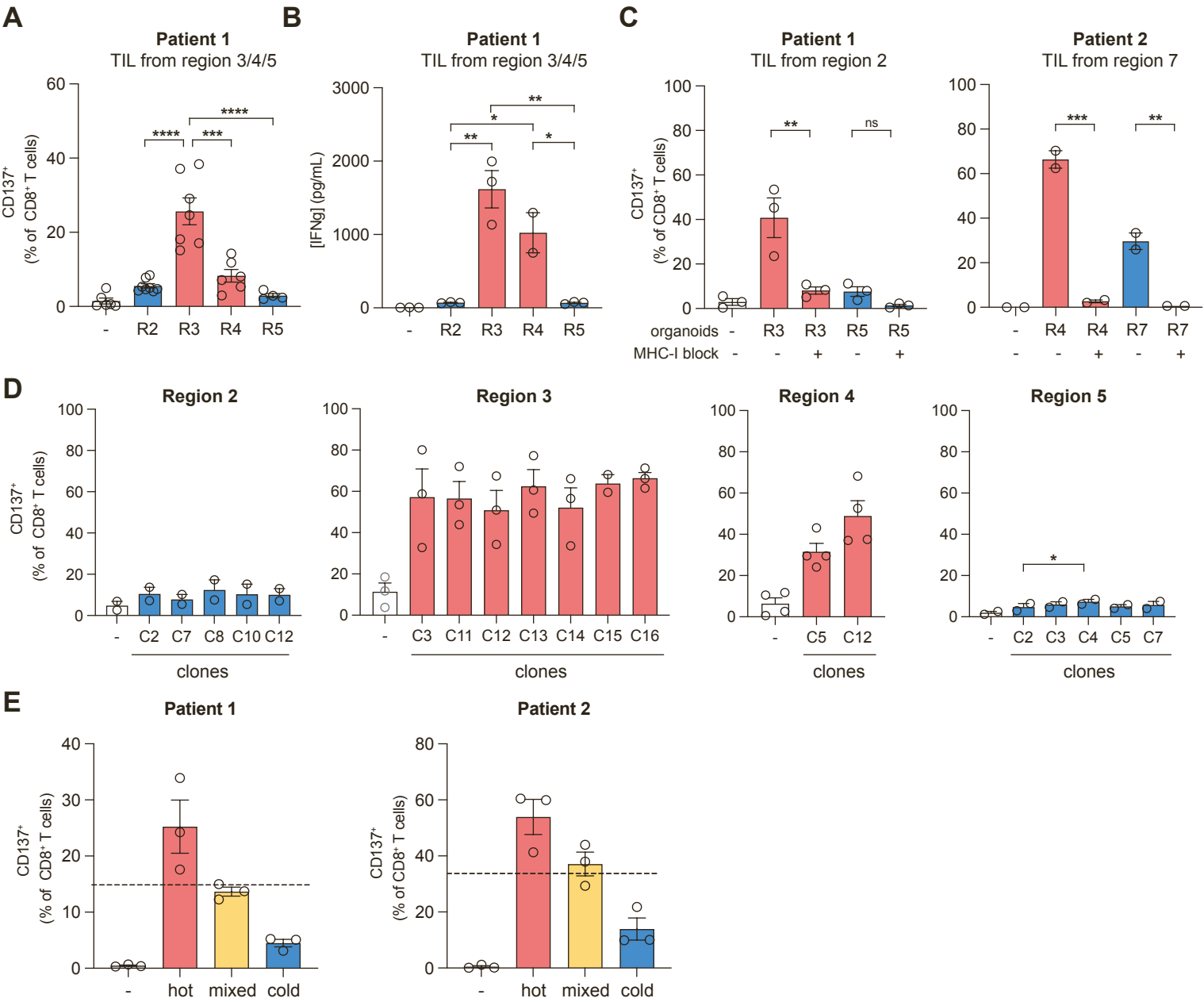


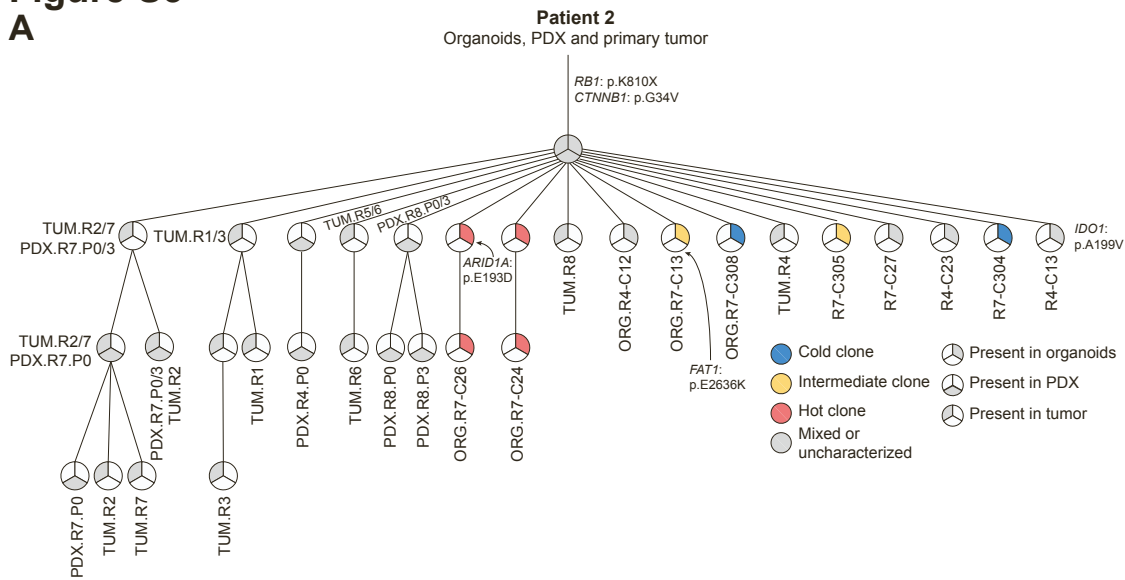
Figure S2. Reactivity of expanded TIL to regional and intraregional clonal organoid sublines, related to Figure 2.

- A) Reactivity of expanded TIL (from regions 3/4/5) to regional organoids (mixed-effects model, $n = 4-8$).
- B) Quantification of secreted IFN γ in supernatant of co-cultures from panel A (mixed effects model, $n = 2-3$ depending on supernatant availability).
- C) Reactivity of expanded TIL to regional organoids \pm W6/32 MHC-I blocking antibody. Data of patient 2 organoids without MHC-I blocking antibodies is also shown in Figure 2B. Repeated-measures ANOVA with Šidák's multiple comparison test, comparing with vs without MHC-I block for each organoid line ($n = 2-3$).
- D) Reactivity of expanded TIL originating from region 2 to intraregional clonal organoid lines. Regions 2 and 5: repeated measures ANOVA ($n = 2$); region 3: mixed-effects model ($n = 2-3$); region 4: paired t-test ($n = 4$).
- E) Reactivity of expanded TIL to hot (patient 1: R3/R4, patient 2: C24/C26) or cold (patient 1: R2/R5, patient 2: C304/C308) clones separately, or equal mixtures of hot and cold clones combined. One-sample t-test comparing mixed condition to average reactivity (dashed line) of hot and cold clones separately ($n = 3$; not significant).

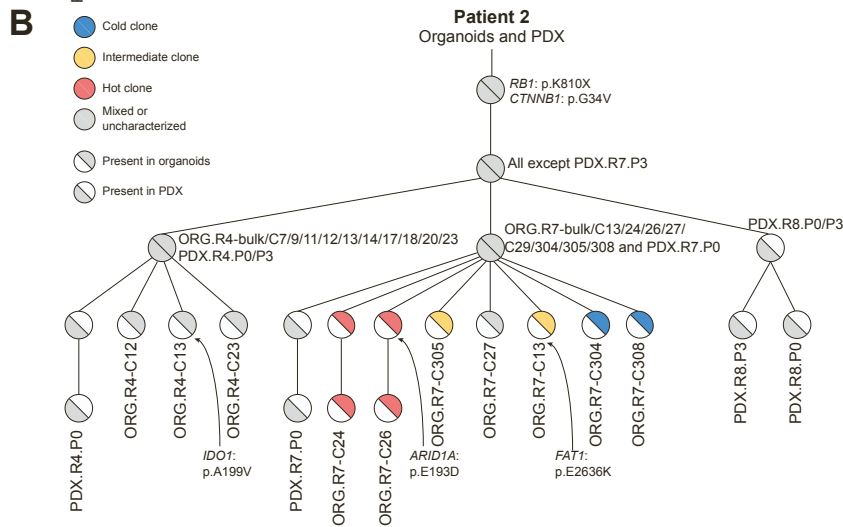
Error bars in all panels show mean \pm S.E.M. Asterisks indicate significance: * $P < 0.05$; ** $P < 0.01$; *** $P < 0.001$; **** $P < 0.0001$.

Figure S3

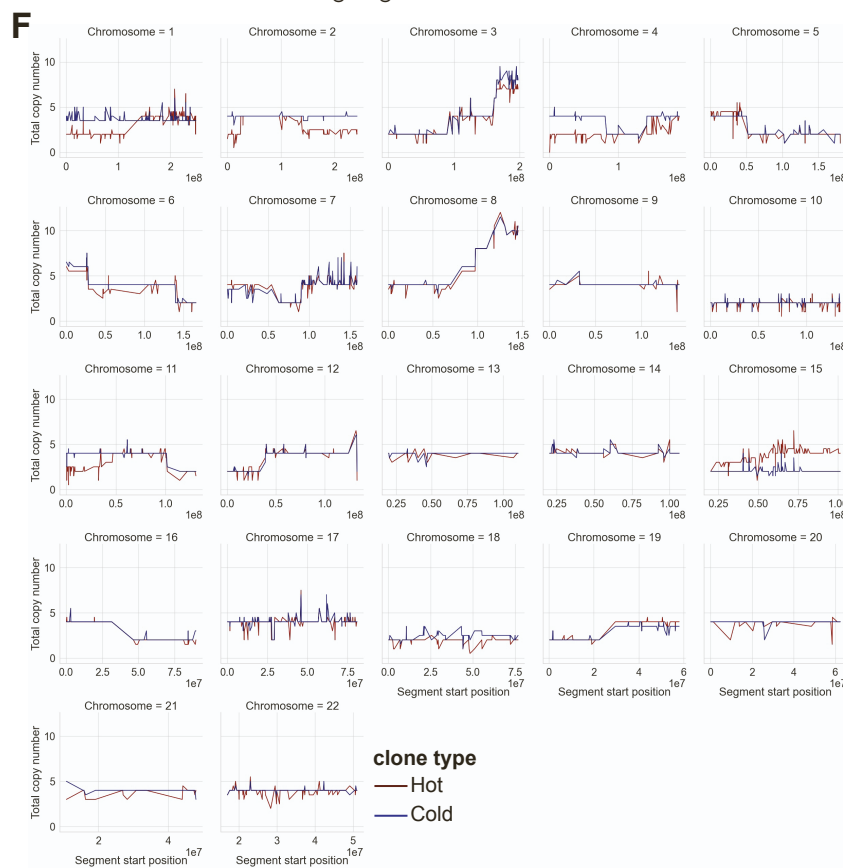
A



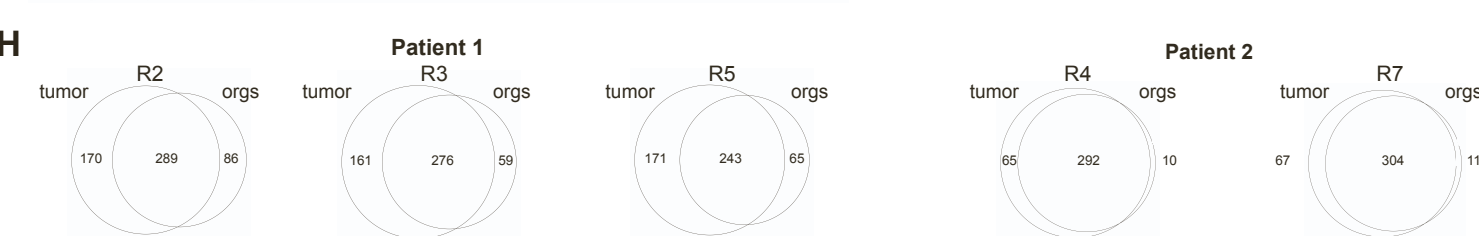
B



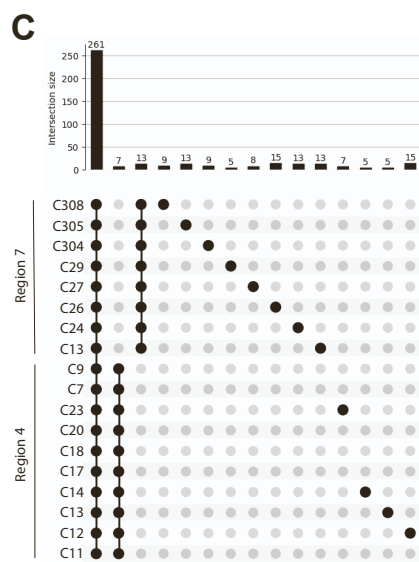
F



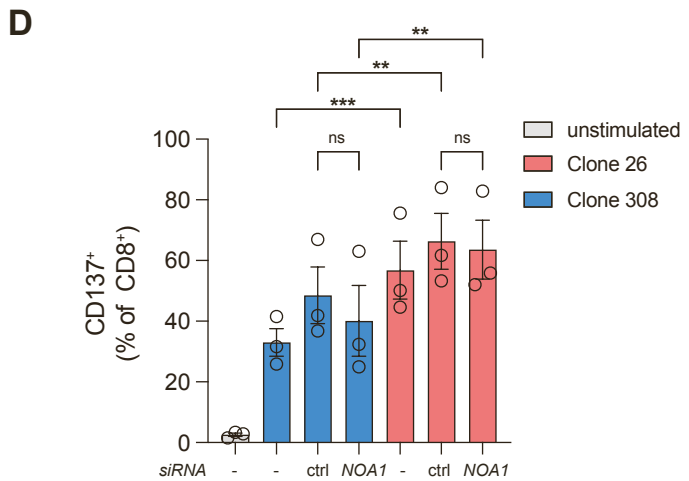
H



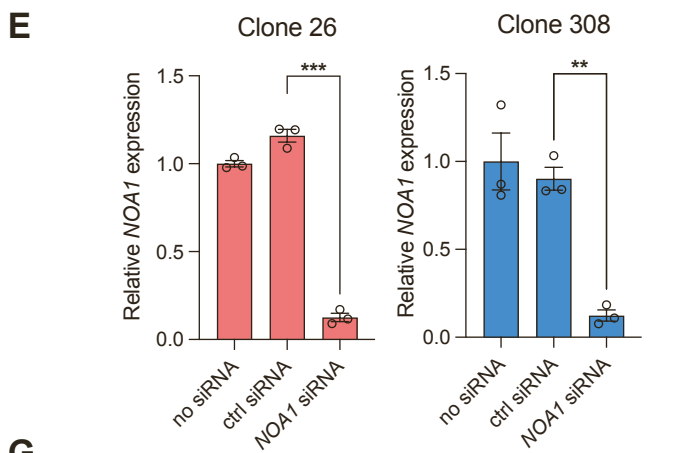
C



D



E



G

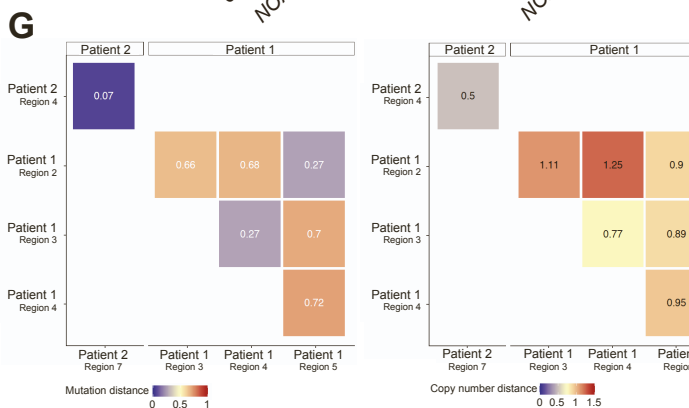


Figure S3. Phylogenetic relationship between intraregional clonal organoid lines from patient 2, related to Figure 3.

- A) Phylogenetic tree based on primary tumor regions, patient-derived xenografts (PDX) and corresponding regional organoid lines from patient 2. Colors indicate immunophenotype based on co-culture data. Nodes labelled by the represented primary tumor region, PDX, or organoid line. Non-synonymous exonic mutations in lung cancer drivers or immune evasion genes (Methods) indicated alongside corresponding nodes. TUM: primary tumor region; ORG: organoid subline; PDX: PDX line with region and passage number.
 - B) As in panel A, but showing tree based on only organoid and PDX sequencing data.
 - C) UpSet plots indicating the number of SNVs shared between intraregional clonal organoid sublines from patient 2. Minimum number of SNVs per group is 5.
 - D) Reactivity of expanded TIL from patient 2 with organoids 48h after transfection with NOA1 or control siRNA. Repeated-measures ANOVA with Šidák's multiple comparison test, comparing indicated conditions (n = 3).
 - E) Expression of *NOA1* based on reverse transcriptase quantitative polymerase chain reaction (RT-qPCR), normalized to the mean expression of *GAPDH* (paired t-test; n = 3).
 - F) Plots showing average copy number along each chromosome for hot (clones 24 and 26) versus cold (clones 304 and 308) from patient 2. X-axis indicates genomic coordinates.
 - G) Mutation and copy number distance for pairwise comparisons of regional organoids from patients 1 and 2. Distance is large if few mutations or copy number alterations are shared, or shared mutations occur at very different cellular frequencies.
 - H) Venn diagrams indicating the number of shared or unique mutations for regional organoids and their corresponding primary tumor regions. Not available for primary tumor region 4 from patient 1 which did not pass copy number quality control due to low tumor purity.
- Error bars in panels D and E show mean \pm S.E.M. Asterisks indicate significance: ** P < 0.01; *** P < 0.001.

Figure S4

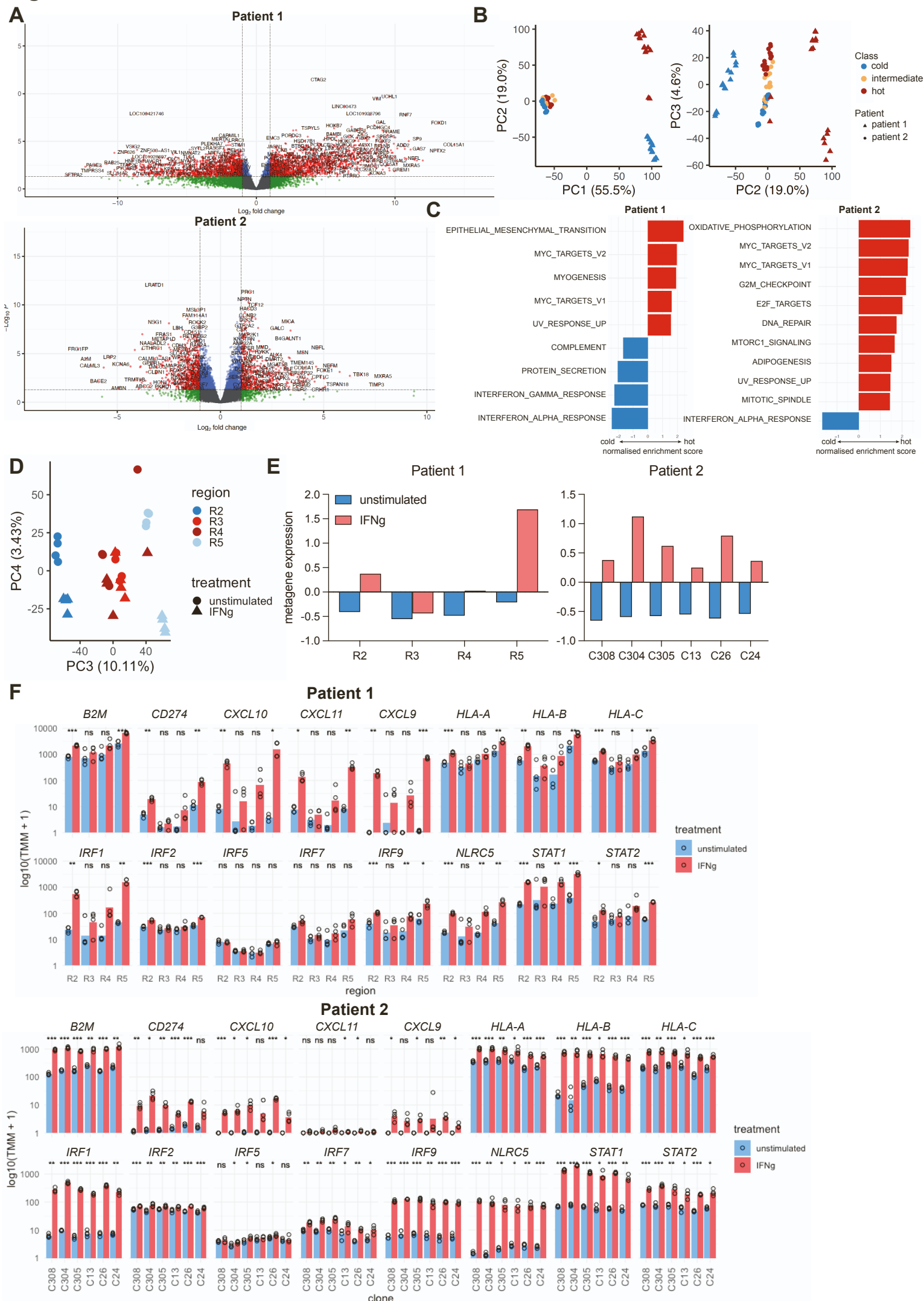
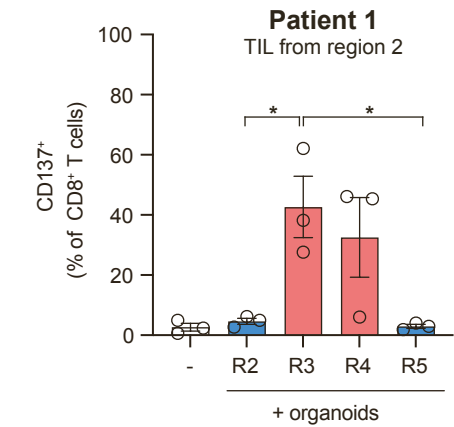


Figure S4. Differential gene expression between cold and hot organoid lines, related to Figure 3.

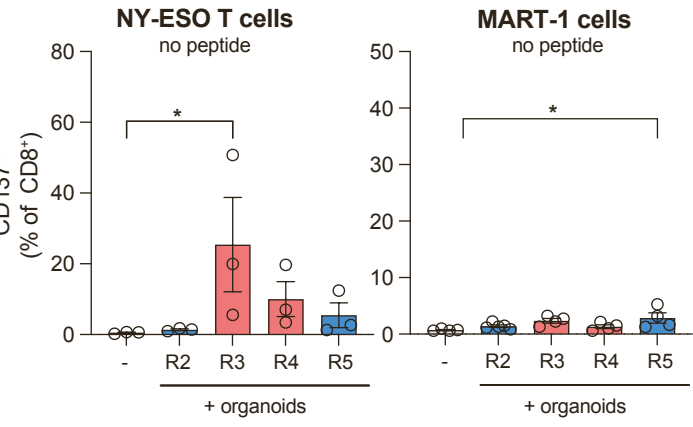
- A) Volcano plots showing differentially expressed genes between cold and hot organoid sublines, annotated by adjusted P value (< 0.05) and absolute log fold change (>1). 2846 genes were significantly differentially expressed in patient 1 and 1113 genes in patient 2. Plot for patient 2 truncated at $\logFC = 10$ (one non-significant data point with $\logFC > 10$ not shown). Significance based on differential expression analysis using limma voom and adjusted for multiple testing using the Benjamini-Hochberg method.
- B) Principal component analysis of organoid sublines from patients 1 and 2 combined in the same plot.
- C) Gene set enrichment analysis of hallmark gene sets based on differential expression data between hot and cold clonal or regional sublines. Only significantly enriched pathways are shown (adjusted P value < 0.05 , Benjamini-Hochberg method).
- D) Principal component analysis (PCA) of RNA sequencing data of regional organoid lines from patient 2 \pm 24h IFNg prestimulation. Numbers along axes indicate percentage of variance explained by principal component 3 or 4.
- E) Induction of metagene expression based on the scaled average expression of all genes part of the "response to interferon gamma" hallmark signature upon IFNg stimulation of organoids for 24h.
- F) Induction of interferon stimulated genes (ISG) for regional or clonal organoid sublines upon stimulation with IFNg for 24h. Asterisks indicate significance for each organoid line \pm IFNg, two-tailed t-test without multiple hypothesis correction ($n = 4$): * $P < 0.05$; ** $P < 0.01$; *** $P < 0.001$.

Figure S5

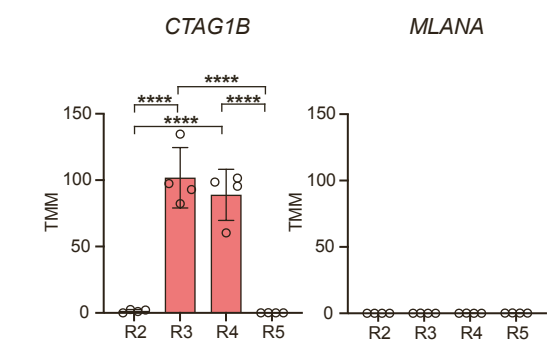
A



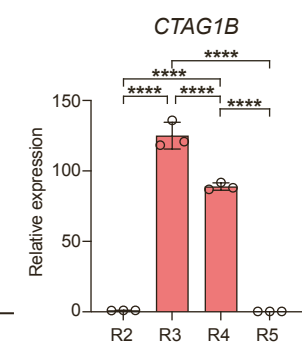
B



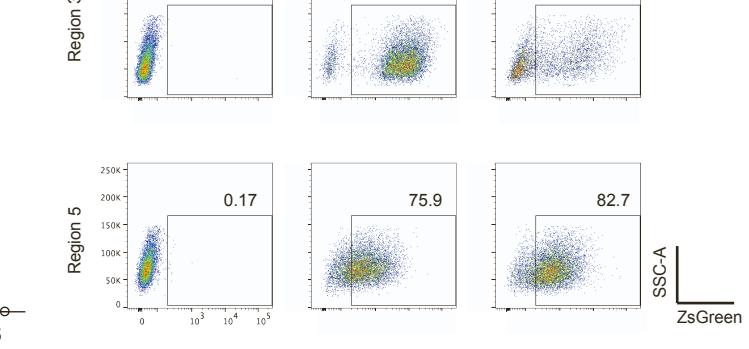
C



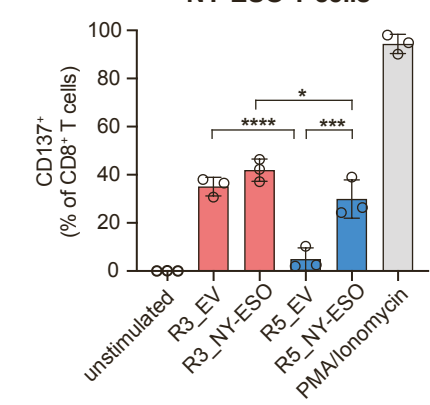
D



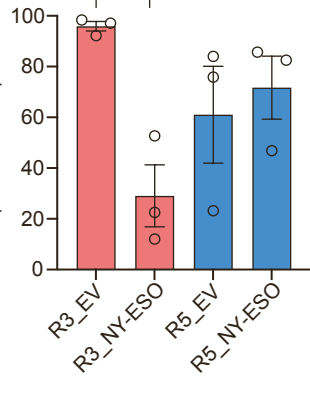
E



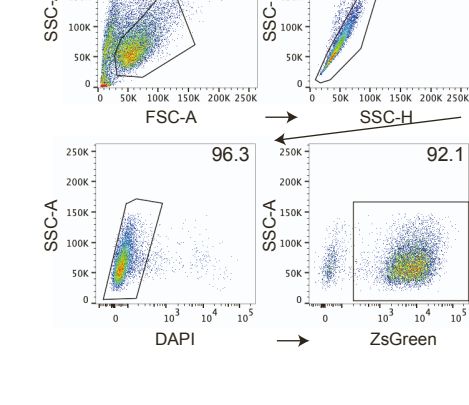
F



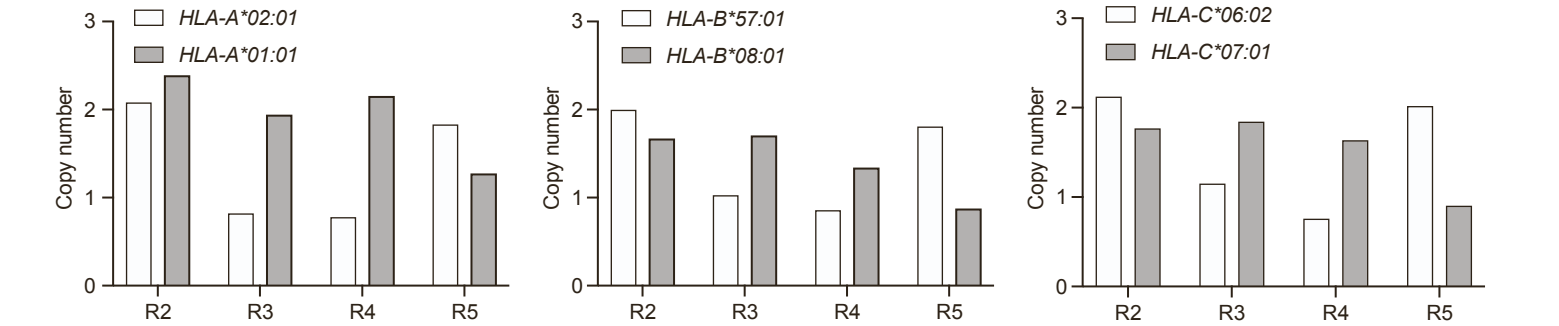
G



H



I



J

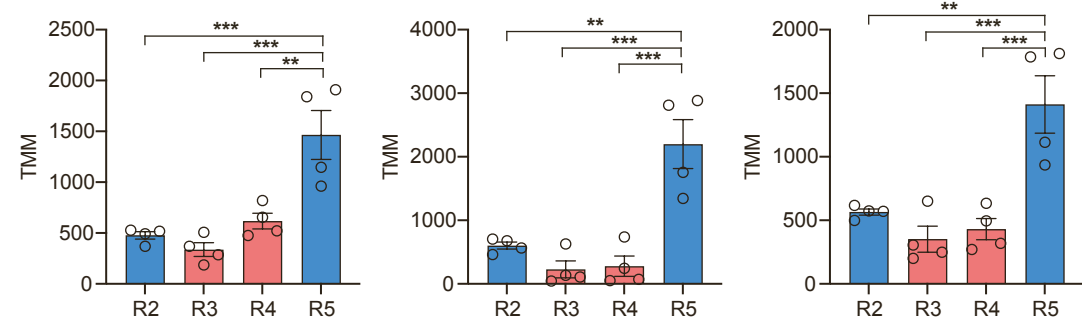


Figure S5. Antigen-dependent subclonal immune evasion, related to Figures 3 and 4.

- A) Reactivity of expanded TIL (from region 2, patient 1) to organoids pre-stimulated with 20 ng/ml IFNg for 48 h (repeated measures ANOVA; n = 3).
- B) Reactivity of NY-ESO- or MART-1-specific T cells to regional organoids from patient 1 in the absence of NY-ESO-1 or MART-1 peptide (statistics: each organoid-stimulated condition compared to unstimulated control, with Dunnet's multiple comparison test; NY-ESO-1: repeated-measures ANOVA, n = 3; MART-1: mixed-effects model, n = 4-5). Unstimulated control is the same as in Figure 4B.
- C) Trimmed normalized mean (TMM) values showing expression of indicated genes in RNA sequencing data of regional organoid sublines (without IFNg) from patient 1 (one-way ANOVA; n = 4).
- D) Expression of CTAG1B based on reverse transcriptase quantitative polymerase chain reaction (RT-qPCR), normalized to the mean expression of three housekeeping genes (HPRT, TBP, UBC). Bars represent mean \pm s.d. and circles indicate individual data points of 3 technical replicates (one-way ANOVA).
- E) Representative flow cytometry plots indicating organoid (patient 1) transduction efficiency of NY-ESO-1 or empty vector based on co-expressed fluorescent protein ZsGreen. Numbers indicate percentage of positive cells.
- F) Reactivity of donor T cells transduced with an NY-ESO-1-specific TCR towards regional organoids (patient 1) transduced with either full-length NY-ESO-1 or empty vector (EV). Repeated-measures ANOVA with Šidák's multiple comparison test, comparing EV versus NY-ESO-1-transduced conditions for each organoid line, or cold versus hot clones for each transduction condition (n = 3).
- G) Transduction efficiency of NY-ESO-1 or empty vector based on the co-expressed fluorescent protein ZsGreen (repeated-measures ANOVA; n = 3).
- H) Gating strategy for determination of transduction efficiency. Numbers indicate percentage of cells of parent population falling in the indicated gate. FSC-A: forward scatter area; SSC-A: side scatter area; SSC-H: side scatter height.
- I) Copy number of HLA class I alleles of patient 1. Copy number represents median copy number of all single nucleotide polymorphisms (SNPs) across the allele.⁴
- J) TMM values showing expression of HLA class I genes in RNA sequencing data of regional organoid sublines (without IFNg) from patient 1 (one-way ANOVA; n = 4).

Error bars in panels A, B, C, F, G, and J show mean \pm S.E.M. Asterisks indicate significance: * P < 0.05; ** P < 0.01; *** P < 0.001; **** P < 0.0001.

Figure S6

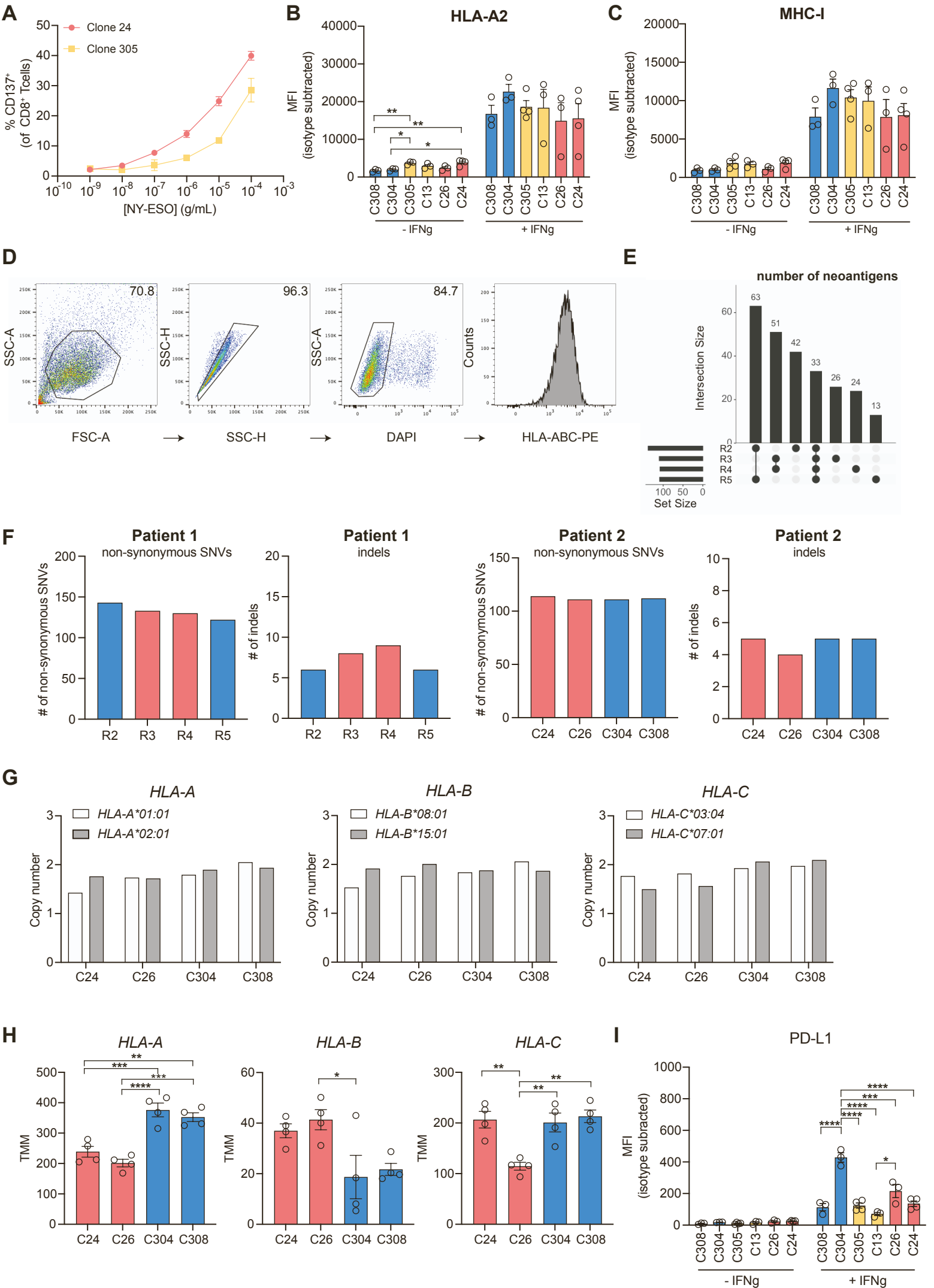


Figure S6. Antigen-independent immune evasion, related to Figures 3 and 4.

- A) Reactivity of NY-ESO-1-specific T cells towards intraregional clonal organoids from patient 2 (region 7), loaded with different concentrations of NY-ESO-1 peptide. Symbols represent mean \pm s.d. of 3 technical replicates.
- B) Organoid cell surface expression of HLA-A2 protein on intraregional clonal organoids from patient 2 (region 7) \pm IFN γ for 24h. MFI: median fluorescence intensity. One-way ANOVA, analysed separately for conditions \pm IFN γ (n = 3-4).
- C) As in (B), showing cell surface expression of pan-MHC-I protein.
- D) Gating strategy for the determination of HLA class I expression levels. Numbers indicate percentage of cells of parent population falling in the indicated gate. FSC-A: forward scatter area; SSC-A: side scatter area; SSC-H: side scatter height.
- E) UpSet plots indicating the overlap of predicted neoantigens between regional organoid lines from patient 1.
- F) Number of non-synonymous SNVs or exonic insertions and deletions (indels) in hot or cold organoid sublines.
- G) Copy number of HLA class I alleles of clonal organoid lines from patient 2 (region 7). Copy number represents median copy number of all single nucleotide polymorphisms (SNPs) across the allele.⁴
- H) Trimmed normalized mean (TMM) values showing expression of HLA class I genes in RNA sequencing data of intraregional clonal organoid sublines from patient 2 (region 7; without IFN γ). One-way ANOVA; n = 4.
- I) As in (B) showing cell surface expression of PD-L1. One-way ANOVA, analysed separately for conditions \pm IFN γ (n = 3-4).

Error bars in panels B, C, H and I show mean \pm S.E.M. Asterisks indicate significance: * P < 0.05; ** P < 0.01; *** P < 0.001; **** P < 0.0001.

Figure S7

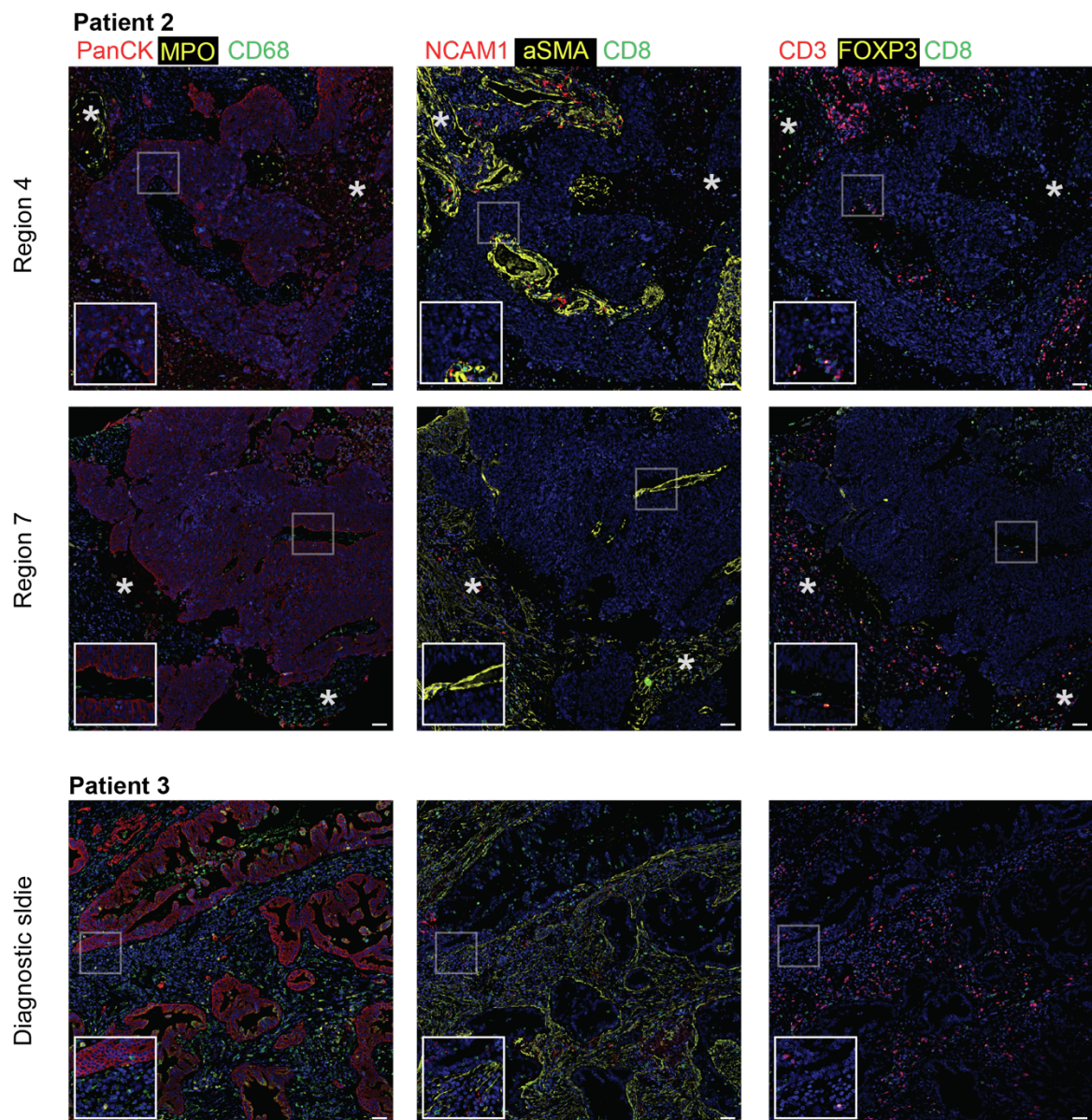


Figure S7. Regional composition of the immune microenvironment for patients 2 and 3, related to Figure 5.

Composite images showing multiplex immunofluorescence staining on serial sections of regions of interest from different tumor regions from patient 2, or of the diagnostic slide for patient 3. Asterisks indicate areas of necrosis. panCK: pan-cytokeratin (epithelial cells); MPO: myeloperoxidase (neutrophils); CD68 (macrophages); NCAM1: neural cell adhesion molecule 1 (NK cells); aSMA: alpha-smooth muscle actin (fibroblasts); CD3 (T cells); FOXP3: forkhead box P3 (regulatory T cells); CD8 (cytotoxic T cells). Scale bar: 200 μm . Lower left insets are 2x magnified corresponding to the boxed area.

Table S2. TIL expansion rates, related to Figure 1.

	Patient 1 (R2 TIL)	Patient 1 (R3/4/5 TIL)	Patient 2 (R7 TIL)	Patient 3 (R1/2/3/4/5 TIL)
Fold expansion pre-REP	24	13,8	0,62	<0,1
Fold expansion REP #1	614	390	51	N/A
Fold expansion REP #2	103	86,7	624	N/A
Fold expansion (cumulative)	1517808	466619	19731	N/A

Table S5. HLA haplotypes, related to Figure 4.

	<i>HLA-A</i>	<i>HLA-B</i>	<i>HLA-C</i>
Patient 1	<i>HLA-A*02:01</i>	<i>HLA-B*57:01</i>	<i>HLA-C*07:01</i>
	<i>HLA-A*01:01</i>	<i>HLA-B*08:01</i>	<i>HLA-C*06:02</i>
Patient 2	<i>HLA-A*02:01</i>	<i>HLA-B*15:01</i>	<i>HLA-C*07:01</i>
	<i>HLA-A*01:01</i>	<i>HLA-B*08:01</i>	<i>HLA-C*03:04</i>

Table S6. Results of linear mixed effects model corresponding to Figure 4E (n = 3-4), related to Figure 4.

Tukey's multiple comparisons test	Summary	Adjusted P Value
C308 vs. C304	ns	0,207
C308 vs. C305	ns	0,1816
C308 vs. C13	***	0,0002
C308 vs. C26	****	<0,0001
C308 vs. C24	****	<0,0001
C304 vs. C305	ns	>0,9999
C304 vs. C13	**	0,0073
C304 vs. C26	**	0,004
C304 vs. C24	****	<0,0001
C305 vs. C13	**	0,0073
C305 vs. C26	**	0,0027
C305 vs. C24	****	<0,0001
C13 vs. C26	ns	0,94
C13 vs. C24	*	0,0162
C26 vs. C24	ns	0,1246

Asterisks indicate significance: * P < 0.05; ** P < 0.01; *** P < 0.001; **** P < 0.0001.

Supplemental references

- [S1]. Lowery, F.J., Krishna, S., Yossef, R., Parikh, N.B., Chatani, P.D., Zacharakis, N., Parkhurst, M.R., Levin, N., Sindiri, S., Sachs, A., et al. (2022). Molecular signatures of antitumor neoantigen-reactive T cells from metastatic human cancers. *Science* 375, 877-884. 10.1126/science.abl5447.
- [S2]. Miller, B.C., Sen, D.R., Al Abosy, R., Bi, K., Virkud, Y.V., LaFleur, M.W., Yates, K.B., Lako, A., Felt, K., Naik, G.S., et al. (2019). Subsets of exhausted CD8(+) T cells differentially mediate tumor control and respond to checkpoint blockade. *Nat Immunol* 20, 326-336. 10.1038/s41590-019-0312-6.
- [S3]. Guo, X., Zhang, Y., Zheng, L., Zheng, C., Song, J., Zhang, Q., Kang, B., Liu, Z., Jin, L., Xing, R., et al. (2018). Global characterization of T cells in non-small-cell lung cancer by single-cell sequencing. *Nat Med* 24, 978-985. 10.1038/s41591-018-0045-3.
- [S4]. Puttick, C., Jones, T.P., Leung, M.M., Galvez-Cancino, F., Liu, J., Varas-Godoy, M., Rowan, A., Pich, O., Martinez-Ruiz, C., Bentham, R., et al. (2024). MHC Hammer reveals genetic and non-genetic HLA disruption in cancer evolution. *Nat Genet* 56, 2121-2131. 10.1038/s41588-024-01883-8.